# HIGH-ENERGY PHYSICS PARTICLE DETECTOR MAGNETS

## THE DEVELOPMENT OF DETECTOR SOLENOIDS

The discovery of type two superconductivity in 1961 (1) was celebrated by the particle physics community. Suddenly it appeared to be possible to create a large volume of magnetic field at an induction not heretofor considered to be economical using conventional magnets. In 1960, one of the largest operating particle detectors using a magnetic field was probably the 72 inch bubble chamber at Berkeley. Within days of the announcement of the discovery of niobium tin as a high field superconductor, particle physicists at Berkeley and other locations set up research groups to make superconducting magnets for particle detectors. There was excitement and constant communication between groups in both the United States and Europe. The cryogenic expertise for the development of the new superconducting magnets came from the people who had developed the cryogenic systems for hydrogen bubble chambers.

The hype and hopes of type two superconductivity soon faded with the realization that the niobium tin then available was not a usable superconductor for large magnets. Early on the experimental work shifted to Nb–Ti and Nb–Zr alloys. Before 1964, Nb–Zr was the alloy of choice because it was more stable than Nb–Ti. The alloy superconductors that performed well in short samples would reach only 30% or 50% of their critical current in a magnet (2). Wires plated with copper appeared to perform somewhat better than bare wire (3). Degradation due to flux jumps was the topic of the day. Improvements in magnet performance were not spectacular because there was no general understanding of what was happening within the superconductor. By 1964, the construction of large superconducting particle detector magnets appeared to be nearly hopeless.

### Early Superconducting Detector Magnets

The paper on cryogenic stability of superconductors by Stekly and Zar (4) caused excitement in the particle physics community. The paper stated that if the superconductor was put in a low resistivity matrix, it didn't matter whether the superconductor flux jumped as long as the matrix remained at a temperature below the superconductor critical temperature. The discovery of cryogenic stability led to the first large detector magnets being built for particle physics. The first of these magnets was the 12 foot bubble chamber magnet at Argonne in 1969 (5,6). The 12 foot bubble chamber was followed by a 7 foot bubble chamber magnet at Brookhaven in 1970 (7), a 15 foot bubble chamber at the Fermilab 1973 (8), a 3.8 meter bubble chamber at CERN 1973 (8,9), the LASS magnet at SLAC 1974 (10), and a number of smaller devices. In 1972, M. Morpugo tested a hollow conductor, forced-cooled, cryostable solenoid for the OMEGA experiment at CERN (11,12). Cryostability solved the scale problem for large superconducting magnets, but magnets built in this way operated at low current densities and were far from being thin from the standpoint of particle transmission through the magnet.

### Low Mass Thin Detector Magnets

Truly thin detector solenoids required a superconductor that could operate at higher current densities without flux jumping. Work by Bean et al. (13), Hancox (14), Chester (15), and Smith et al. (16,17) paved the way to understanding the intrinsic stability of superconductors, which led to the development of modern, twisted multifilamentary conductors with a low matrix metal to superconductor ratio. Increasing the current density in the magnet winding was one way of making the magnet more transparent to particles.

In addition, thin superconducting solenoids had to be cooled in a different way. Helium bath cryostats contain too much material for them to be transparent to particles. In order to reduce the mass of the cryostat, it was found that thin solenoids had to be cooled indirectly by conduction to tubes that contain helium. Experimental work in the 1970s suggested that two-phase helium cooling would result in a lower operating temperature than supercritical helium cooling (18).

The first experiment calling for a thin solenoid was at the ISR at CERN (19). In 1975 a thin solenoid was proposed for the MINIMAG experiment proposed by the Lawrence Berke-

**Table 1. Parameters for Various Thin Superconducting Detector Solenoids**

| Magnet | Central Induction (T) | Warm Bore Diameter (m) | Cryostat Length (m) | Matrix Material | Conductor Location | Radiation Thickness (Rad Len) | Stored Energy (MJ) | Matrix $J$ (A mm$^{-2}$) | Type of Cooling |
|---|---|---|---|---|---|---|---|---|---|
| CLEO-1 | 1.5 | 2.0 | 3.7 | Cu | Outside | 0.7 | 10.0 | ~350 | Forced |
| PEP-4 | 1.5 | 2.04 | 3.84 | Cu | Outside | 0.83 | 10.9 | 645 | Forced |
| CELLO | 1.3 | 1.5 | 4.02 | Al | Outside | 0.6 | 5.0 | — | Forced |
| CDF | 1.5 | 2.85 | 5.4 | Al | Inside | 0.84 | 30 | 64 | Forced |
| TOPAZ | 1.2 | 2.72 | 5.4 | Al | Inside | 0.70 | 20 | 56 | Forced |
| VENUS | 0.75 | 3.4 | 5.6 | Al | Inside | 0.52 | 12.0 | ? | Forced |
| ALEPH | 1.5 | 4.96 | 7.0 | Al | Inside | 1.6 | 136 | 30.8 | Natural |
| AMY | 3.0 | 2.39 | 2.11 | Al | Outside | >2 | 40 | 50 | Pool |
| GSI | 0.6 | 2.4 | 3.3 | Al | Inside | ~1.0 | 3.4 | — | Natural |
| ZEUS | 1.8 | 1.72 | 2.9 | Al | Inside | >2 | 16 | ? | Forced |
| DELPHI | 1.2 | 5.2 | 7.4 | Al | Inside | 1.7 | 108 | 46.3 | Forced |
| H-1 | 1.2 | 5.2 | 6.0 | Al | Inside | 1.8 | 130 | 46 | Forced |
| CLEO-2 | 1.5 | 2.9 | 3.8 | Al | Inside | 2.2 | 25 | 41.3 | Natural |
| g-2 | 1.45 | 14.1[a] | 0.18[b] | Al | Inside | >2 | 5.5 | 81.8 | Forced |
| KEK Balloon | 1.2 | 0.852 | 2.0 | Al | Inside | 0.21 | 0.815 | 241 | Pool at End |
| SDC Test Coil | 1.5 | 1.7 | 2.4 | Al | Inside | 1.2 | 45 | 63.4 | Forced |
| BaBar | 1.5 | 2.76 | 3.85 | Al | Inside | <1.4 | 23 | 37 & 67 | Natural |
| CMS | ~4.0 | ~6.0 | 12.5 | Al | Inside | >2 | 2500 | 15.4 | Natural |

[a]Beam orbit diameter, outer solenoid coil diameter = 15.1 m, inner solenoid coil diameter = 13.4 m.
[b]Total gap between the iron poles (the iron return path is C-shaped, the total gap in the iron is about 0.23 m.

ley Laboratory in 1975 (20). This experiment required a one meter diameter solenoid that was 0.35 radiation lengths thick, including the cryostat. Two 1 m diameter test coils were built and tested in 1975 and 1976 (21,22). The conductor in the test coils was operated at matrix plus superconductor current densities as high as 1250 A mm$^{-2}$. The MINIMAG experiment was not built, but a larger detector for an experiment at PEP colliding beam ring at the SLAC was embarked upon. This detector required a clear bore diameter of 2 m with a gap of 3.3 m between the iron poles. A uniform 1.5 T induction (better than 1 part in 1000 within a 2 m diameter, 2 m long volume) was required. The coil and cryostat had to be less than 0.7 radiation lengths thick so that calorimeters and muon detectors could be located outside of the magnet. Work began on a 2 m diameter test coil in late 1976. This coil was tested in 1977 and 1978 (23). The thin coil experimental work at Berkeley led directly to the CLEO-1 detector at Cornell University (19) and the PEP-4 detector (24,25) at the PEP colliding beam facility at the SLAC.

A group at CEN Saclay outside Paris decided to build their detector magnet using a conductor that had a low copper to superconductor ratio soldered to very pure aluminum high residual resistance ratio (RRR) matrix. The advantages of the aluminum matrix were as follows: The minimum propagation zone was lengthened so that the energy needed to induce a quench in the magnet was increased by over three orders of magnitude, and the quench propagation velocity along the wire was faster than for a comparable copper matrix conductor. The 2 m diameter CELLO detector magnet was first tested in 1979 (26). A conductor made with the copper matrix superconductor coextruded in pure aluminum (RRR > 1000) was developed in a number of locations at about the same time (27). This type of conductor was used on the CDF detector magnet at Fermilab (28), on the VENUS detector (29), the TOPAZ (30) detector, and the AMY detector (31) at KEK in Japan, on the ALEPH (32) and DELPHI (33) detectors at CERN, on the H-1 (34) and ZEUS (35) detectors at DESY in Germany, on the GSI solenoid (36) at Darmstadt, on the CLEO-2 detector (37) at Cornell University, and on the CLOE detector at Frascati. A thin solenoid SDC experiment test coil was tested before the SSC was canceled (38). The Japanese flew a 1 m diameter balloon solenoid (39,40) that used a low matrix to superconductor ratio RRR ≥ 1000 aluminum matrix conductor to achieve a very low radiation thickness (about 0.25 radiation lengths) for a cosmic ray experiment. Detector solenoids for the BaBar (41) experiment at the B factory at SLAC, the ATLAS (42,43) toroidal magnet detector at the LHC, and the CMS (44) solenoidal detector at the LHC are currently under development or construction. All of these magnets will use a pure aluminum matrix superconductor that will be wound on the inside of a hard aluminum support structure.

The use of thin solenoid magnet construction techniques has proven to be less costly even when thinness was not required. As a result, the thin detector solenoid construction techniques were used to build two 13.4 m diameter and one 15.1 m diameter solenoid for the g-2 experiment at the Brookhaven National Laboratory (45). These solenoids were successfully tested to full field in the summer of 1996 (46). Table 1 summarizes the design parameters for a number of the thin superconducting detector magnets.

## THE DEFINING PARAMETERS FOR THIN SOLENOIDS

In the literature, thinness is defined in terms of interaction lengths, absorption lengths, and radiation lengths. In high-energy physics detectors, there is no one universal definition of thinness. Thus, discussion of interaction lengths must identify the particle, and absorption lengths must identify the particle and its energy. The most common definition of thinness uses radiation lengths as a defining parameter. One ra-

diation length occurs when 63.2% $(1 - 1/e)$ of the neutral particles have formed charged particle pairs. This definition is appropriate in many experiments because the calorimeters and muon detectors are the only detectors that are located outside the magnet.

The physical thickness of a material that is one radiation length thick is a function of the material atomic number $Z$ and the material specific density $\gamma$. In order for a superconducting magnet to be thin, it must be made from low-density, low-$Z$ materials. The radiation thickness of a detector magnet is the sum of the radiation thicknesses of the windings, the coil support structure, the cryostat, and the intermediate temperature shields.

The radiation thickness $X_0$ of a magnet component can be estimated using the following expression:

$$X_0 = \frac{t}{L_r \cos(\alpha)} \tag{1}$$

where $X_0$ is the radiation thickness of the magnet component (given in radiation lengths), $t$ is the physical thickness of the material in the magnet component, $L_r$ is the thickness for one radiation length of the material in the magnet component, and $\alpha$ is the particle angle with respect to a line perpendicular to the component. In most cases, radiation thickness is defined when $\alpha = 0$.

The value of $L_r$ used in Eq. (1) can be obtained from Table 2 (47,48) or it can be estimated using the following expression:

$$L_r = 158\frac{Z^{-0.73}}{\gamma} \tag{2}$$

where $Z$ is the atomic number for the heaviest element in the compound that makes up the component and $\gamma$ is the mass specific density for the material in the component. For pure elements, Eq. (2) yields a good estimate of $L_r$, except for ordinary hydrogen, which has no neutrons in its nucleus. For components made from compounds, the use of the $Z$ for the heaviest element in the compound will tend to overestimate radiation thickness whereas using an average value of $Z$ will

**Table 2. The Radiation Thickness of Various Materials**

| Material | $Z$ | Mass Density (kg m$^{-3}$) | One Radiation Length $L_{rad}$ | |
|---|---|---|---|---|
| | | | kg m$^{-2}$ | mm |
| Pure elements | | | | |
| Hydrogen | 1 | 70.8[a] | 630.5 | 8,900 |
| Deuterium | 1 | 163[a] | 1,261.0 | 7,640 |
| Helium | 2 | 125[a] | 943.2 | 7,550 |
| Lithium | 3 | 534 | 827.6 | 1,550 |
| Beryllium | 4 | 1,848 | 651.9 | 353 |
| Boron | 5 | 2,370[b] | 553.9 | 234 |
| Carbon | 6 | ~1,550[b] | 427.0 | ~275 |
| Nitrogen | 7 | 808[a] | 379.9 | 470 |
| Oxygen | 8 | 1,142[a] | 344.6 | 302 |
| Neon | 10 | 1,207[a] | 289.4 | 240 |
| Magnesium | 12 | 1,740 | 254.6 | 146 |
| Aluminum | 13 | 2,700 | 240.1 | 88.9 |
| Argon | 18 | 1,400[a] | 195.5 | 140.0 |
| Titanium | 22 | 4,540 | 168.7 | 37.2 |
| Chromium | 24 | 7,200 | 146.7 | 20.4 |
| Iron | 26 | 7,870 | 138.4 | 17.6 |
| Nickel | 28 | 8,902 | 131.9 | 14.8 |
| Copper | 29 | 8,960 | 128.6 | 14.3 |
| Niobium | 41 | 8,570 | ~101 | ~11.8 |
| Tin | 50 | 7,310 | 88.6 | 12.1 |
| Tungsten | 74 | 19,300 | 67.6 | 3.5 |
| Lead | 82 | 11,350 | 63.7 | 5.6 |
| Uranium | 92 | 18,950 | 60.0 | 3.2 |
| Compounds, Alloys and Other Materials | | | | |
| Water | | 1,000[a] | 360.8 | 360.8 |
| Polyethylene | | ~950 | 447.8 | ~470 |
| Epoxy resin | | ~1,450 | ~406 | ~280 |
| Glass fiber epoxy | | ~1,750 | ~330 | ~189 |
| Carbon fiber epoxy | | ~1,600 | ~418 | ~261 |
| Boron aluminum (45% B) | | 2,550 | ~381 | ~149 |
| Mylar | | ~1,390 | 399.5 | 287 |
| Sodium iodide | | 3,670 | 94.9 | 25.9 |
| Lithium floride | | 2,640 | 392.5 | 149 |
| 304 Stainless steel | | 7,900 | 137.9 | 17.4 |
| Nb–47% Ti | | 6,520 | 132.8 | 20.4 |

[a]Liquid state.
[b]Graphite or carbon fiber.

often underestimate the radiation thickness. For components made from alloys or composites, the method of mixtures can be applied to achieve a good estimate of $L_r$.

## THIN DETECTOR SOLENOID DESIGN CRITERIA

The strategy for minimizing the radiation thickness of a superconducting detector magnet requires the following steps: (1) Massive parts such as current bus bars, gas-cooled electrical leads, cold mass support structures, vacuum services, and cryogenic services should be located at the ends of the magnet away from the region that is supposed to have a minimum radiation thickness. (2) The superconductor should have a minimum amount of copper and niobium titanium. The stabilizer matrix material for the superconductor should be made of a low-resistivity, low-$Z$ material such as ultrapure aluminum. (3) The support structure on the outside of the coil, which will carry the hoop forces in the solenoid, should be made from a strong, ductile, low-$Z$, low-density material with a high thermal conductivity. (4) The magnet should be cooled indirectly with helium in tubes that are attached to the coil support structure. (5) Intermediate temperature shields for the cryostat should be made of a low-$Z$, low-density, high thermal conductivity material such as aluminum. (6) The inner cryostat vacuum vessel should be made from a strong low-$Z$, low-density material. (7) The outer cylinder of the cryostat vacuum vessel should be made from a material with a low-$Z$, a low density, and an elastic modulus that is reasonably high.

The typical physics detector solenoid is usually between two unsaturated iron poles that have an average relative permeability that is greater than 20. The magnetic flux generated by the solenoid winding is returned by an iron yoke that carries the magnetic flux from one pole to the other. The relative permeability of the iron in the return yoke is usually above 50. Figure 1 shows a typical thin detector solenoid within an experiment located around the collision point of colliding beam storage ring. The number of ampere turns needed to generate a uniform magnetic induction within the detector solenoid can be estimated by using the following expression (49):

$$NI = \frac{B_0 L_g}{\mu_0} \tag{3}$$

where $NI$ is the total number of ampere turns in the detector solenoid coil needed to generate a magnetic induction $B_0$ in a solenoid that has unsaturated iron poles that are a distance $L_g$ apart. $\mu_0$ is the permeability of air ($\mu_0 = 4\pi \times 10^{-7}$ H m$^{-1}$).

Equation (3) underestimates the ampere turns needed to generate the magnetic induction in the solenoid bore anywhere from 3% to 30% depending on the design of the magnetic circuit and the central induction within the solenoid. The equation underestimates the required ampere turns because the relative permeability of the iron in the poles and the return yoke is not infinite and the iron in the pole pieces is often segmented, with detectors between the segments. Often the extra ampere turns are put at the ends of the solenoid so that the desired field uniformity within the solenoid can be achieved. Computer codes such as POISSON (50) and OPERA2D (51) can be used to determine the number of ampere turns needed to generate the desired central induction and the desired field uniformity within the detector volume.

The amount of superconductor needed to generate the magnetic field is quite small. When Nb–Ti with a critical current density of 2500 A mm$^{-2}$ at 4.2 K and 5.0 T is used, about 0.3 mm of Nb–Ti is needed for every tesla of central magnetic induction produced (52). The copper to superconductor ratio for the conductor can be as low as 0.8. The amount of stabilizer (usually annealed 0.99999 pure RRR $>$ 1000 aluminum) in the conductor is dictated by the type of quench protection chosen.

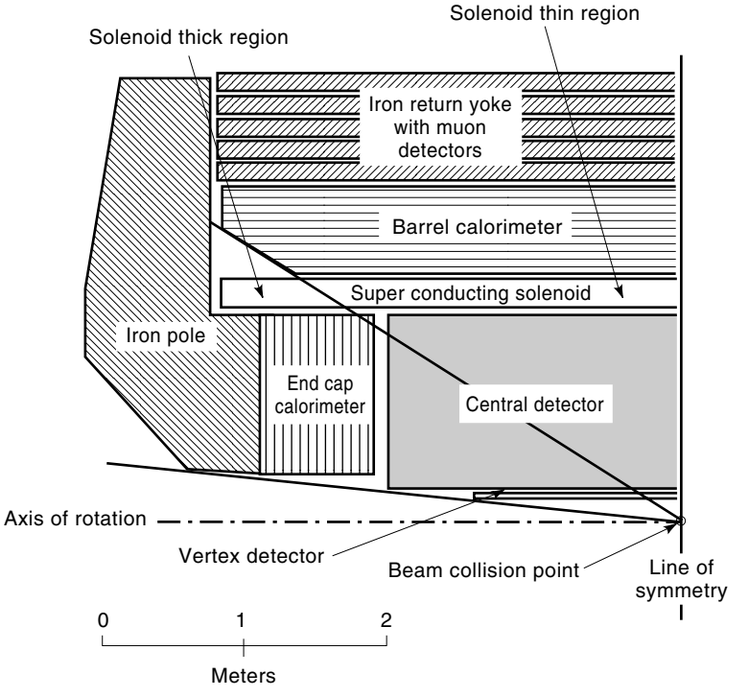


**Figure 1.** A quarter section view of a typical colliding beam physics detector with the solenoid cryostat shown. (The thin and thick sections of the superconducting magnet are shown.)

The physical thickness of the superconducting coil is determined by the thickness of stabilizing matrix material in the conductor. The average conductor current density $J_m$ is determined by the safe quench condition for the coil. For safe magnet quenching through a dump resistor, the magnet $E_0 J_m^2$ limit can be estimated using the following expression (53,54):

$$E_0 J_m^2 = V I_0 F^*(T_m) \frac{r}{r+1} \tag{4}$$

where $E_0$ is the magnet stored energy when it is operated at its design current $I_0$, $V$ is the discharge voltage for the magnet during the quench (for large magnets $V$ is limited to about 500 V), $I_0$ is the magnet design current ($I_0$ is typically greater than 3000 A), $r$ is the matrix to superconductor ratio, and $F^*(T_m)$ is the integral of $J_m^2\, dt$ needed to raise the stabilizer adiabatic hot spot temperature from 4 K to a maximum hot spot temperature $T_m$. (For RRR = 1000 aluminum, $F^*(T_m) = 6 \times 10^{16}$) $A^2\ m^{-4}$ when $T_m = 300$ K.)

The magnet stored energy $E_0$ can be estimated if one knows the solenoid coil diameter $D_c$, the central induction $B_0$, and the gap between the iron poles $L_g$. An approximate expression for the magnet stored energy is as follows:

$$E_0 = \frac{\pi D_c^2 B_0^2 L_g}{8\mu_0} \tag{5}$$

If the $E_0 J_m^2$ limit for the magnet is increased, then the magnet design current $I_0$ or the magnet discharge voltage $V$ must be increased as well. Quench back from the coil support structure can be helpful in improving the quench protection for the magnet. Magnets that employ quench back (22,55) as the primary means for quench protection can be operated at a much higher $E_0 J_m^2$ limit, but the typical solenoid that is protected with a dump resistor across the leads has the $E_0 J_m^2$ limit given by Eq. (4).

From Eqs. (4) and (5), one can determine the thickness of the superconducting coil $t_c$ using the following expression:

$$t_c = \left( \frac{\pi D_c^2 B_0^4 L_g}{8\mu_0^3 V I_0 F^*(T_m) \dfrac{r}{r+1}} \right)^{0.5} \tag{6}$$

In order for the coil thickness to be thinner than the value given by Eq. (6), quench back must turn the whole coil normal in a time that is significantly faster than the $L$ over $R$ time constant of the coil and dump resistor circuit.

In virtually all of the large detector solenoids, the superconducting coil is wound inside the support cylinder (56). When the coil is inside the support cylinder, the joint between the coil and the support structure is in compression as the magnet is charged. An additional advantage is that the coil package cools down from the outside. Thus, the support cylinder shrinks over the coil. A few of the smaller detector magnets were wound with the coil on the outside of a bobbin or support cylinder. In all these cases, the conductor was designed to carry all of the magnetic hoop forces and the helium cooling tubes were attached to the outside of the coil. The superconducting solenoid coil can be wound in one or two layers. A two-layer coil has the advantage of having both leads from the coil come out at the same end of the coil package. There are a number of accepted ways of winding coils so that they have more current per unit length at the solenoid ends than in the center. One approach is to make the matrix current density higher at the ends by making the conductor thinner along the coil axis.

The thickness of the support shell outside the superconducting coil is governed by the magnetic pressure on the coil windings (49). Total strain of the coil should be limited to prevent plastic deformation of the conductor matrix. If the conductor has a pure aluminum matrix, the strain limit for the coil should be set to about 0.1% (57,58). A conservative view assumes that virtually all of the magnetic forces are carried by the support shell, and the calculated shell thickness is given by the following expression:

$$t_s = 250 \frac{B_0^2 D_s}{\mu_0 E_s} \tag{7}$$

where $t_s$ is the design thickness for the support shell, $D_s$ is the inside diameter of the support shell, and $E_s$ is the modulus of elasticity of the material in the support shell. If the superconductor is included in the overall strain calculation, the thickness of the support shell can be reduced.

The coil cryostat is primarily the vacuum vessel that provides the insulating vacuum for the magnet. The two primary cryostat elements are the outer cryostat vacuum vessels and the warm bore tube. The multilayer insulation and shields make up only a minor part of the cryostat's radiation thickness. A design thickness of a solid outer cryostat wall can be calculated using the following expression, which has been derived from the equation for elastic buckling of a cylinder under external pressures (59,60):

$$t_0 = 1.08 \left( \frac{P_0 L_0 D_0^{1.5}}{E_0} \right)^{0.4} \tag{8}$$

where $t_0$ is the thickness of the outer cryostat wall, $P_0$ is pressure on the outer wall of the cryostat (usually $P_0 = 1$ atm $= 1.013 \times 10^5$ Pa), $L_0$ is the length of the thin unsupported section of the outer cryostat wall, $D_0$ is the diameter of the outer cryostat wall, and $E_0$ is the elastic modulus of the material in the outer wall of the cryostat.

The minimum thickness of the inner wall of the cryostat can be derived if one knows the design ultimate stress for the material in the inner wall (58,61). The margin of safety normally applied to a pressure vessel wall, such as the cryostat inner wall, is usually four (62). An expression for the minimum inner cryostat wall thickness is given as follows:

$$t_i = 2 \frac{P_i D_i}{\sigma_u} \tag{9}$$

where $t_i$ is the minimum wall thickness for the inner cryostat wall, $P_i$ is the design internal pressure on the inner cryostat wall, $D_i$ is the diameter of the inner cryostat wall, and $\sigma_u$ is the ultimate stress for the material used in the inner cryostat wall. Sometimes, the cryostat inner wall thickness is greater than the thickness given by Eq. (9) so that one can mount particle detectors and other equipment on this wall.

The material thicknesses calculated using Eq. (6)–(9) can be used to estimate the radiation thickness of the detector solenoid. Table 3 compares four cases where the coil diameter,

**Table 3. A Comparison of Four Thin Solenoids**

| Component | Case 1 | Case 2 | Case 3 | Case 4 |
|---|---|---|---|---|
| Central induction $B_0$ (T) | 1.5 | 1.5 | 0.75 | 1.5 |
| Solenoid coil diameter (m) | 2.0 | 4.0 | 4.0 | 4.0 |
| Gap between the iron poles (m) | 3.3 | 6.6 | 6.6 | 3.3 |
| Length of the solenoid thin section (m) | 3.3 | 6.6 | 6.6 | 3.3 |
| Cryostat inside diameter (m) | 1.84 | 3.80 | 3.80 | 3.80 |
| Cryostat outside diameter (m) | 2.24 | 4.28 | 4.22 | 4.26 |
| Cryostat overall length (m) | 3.85 | 7.30 | 7.30 | 3.85 |
| Magnet ampere turns (MA) | 3.94 | 7.88 | 3.94 | 3.94 |
| Magnet stored energy (MJ) | 9.28 | 74.25 | 18.56 | 37.13 |
| Magnet design current (A) | 5000 | 5000 | 5000 | 5000 |
| Magnet self–inductance (H) | 0.74 | 5.94 | 1.48 | 2.97 |
| Number of conductor layers | 2 | 2 | 2 | 2 |
| Number of coil turns | 788 | 1576 | 788 | 788 |
| Quench discharge voltage (V) | 500 | 500 | 500 | 500 |
| Matrix current density (A mm$^{-2}$) | 127.1 | 44.9 | 89.9 | 63.6 |
| Nb–Ti plus copper thickness (mm) | 0.90 | 0.90 | 0.45 | 0.90 |
| Total coil thickness (mm) | 9.39 | 26.58 | 13.28 | 18.75 |
| Coil support structure thickness (mm) | 12.97 | 25.95 | 6.49 | 25.95 |
| Inner cryostat thickness (mm) | 1.24 | 2.57 | 2.57 | 2.57 |
| Outer cryostat thickness (mm) | 13.11 | 25.23 | 25.23 | 19.12 |
| Magnet radiation thickness (Rad Len) | 0.495 | 0.974 | 0.589 | 0.829 |
| Magnet cold mass (metric tons) | 2.12 | 14.4 | 6.16 | 7.00 |
| Magnet overall mass (metric tons) | 4.00 | 23.5 | 15.3 | 11.8 |

the gap between the iron poles, and the central induction are varied. In all four cases, the cryostat walls and coil support structure are made from solid aluminum. The superconductor is Nb–Ti with a thick aluminum stabilizer. The assumed insulation system inside and outside the cold mass consists of 60 layers of aluminized mylar and netting with a single 1 mm thick aluminum shield on other side of the coil. Figure 2 shows a cross section of a coil and cryostat for CASE 2 given in Table 3. In order to make a significant reduction in the radiation thicknesses shown in Table 3, quench back must be the primary mode of quench protection and the outer cryostat vacuum vessel must be made from a cellular (honeycomb) composite structure that is physically thicker than a solid aluminum vessel (63,64).

## MAGNET POWER SUPPLY AND COIL QUENCH PROTECTION

The power supply parameters are set by the coil charge time $t_{ch}$ and the design operating current $I_0$ for the solenoid. The charge time for a detector solenoid is rarely an issue. Charge times as long as one hour are acceptable. The charge voltage $V = L_1\, di_1/dt$, where $L_1$ is the self-inductance of the magnet circuit; and $di_1/dt$, is the magnet current charge rate. (For a typical magnet, $di_1/dt$, $= I_0/t_{ch}$.) To determine the power supply voltage, one must add the $IR$ voltage drop across the gas-cooled electrical leads and the cables connecting the power supply to the magnet. In addition, a voltage drop of 0.9 V should be allocated to the power supply back wheeling diodes and a current shunt.

### The Quench Protection Dump Resistor

Most large detector magnets are protected by a dump resistor across the gas-cooled electrical leads. When a quench is detected, the power supply is disconnected and the dump resistor is put across the leads. The design of a magnet dump resistor circuit is determined by the following relationship (54):

$$F^*(T_m) = \int_0^\infty j(t)^2\, dt = \frac{r}{(r+1)} \int_{T_0}^{T_m} \frac{C(T)}{\rho(T)}\, dT \qquad (10)$$

where $j(t)$ is the current density in the magnet superconductor cross section as a function of time $t$, $C(T)$ is the superconductor volume specific heat as a function of temperature $T$, $\rho(T)$ is the superconductor matrix material electrical resistivity as a function of temperature, and $r$ is the ratio of matrix material to superconductor in the magnet conductor. $T_0$ is the starting temperature of the magnet (about 4 K), and $T_m$ is the maximum allowable hot spot temperature for the magnet conductor (usually 300–350 K). For a conductor with a very pure aluminum matrix with an RRR of 1000, the value of $F^*(T_m)$ is around $6.0 \times 10^{16}$ A$^2$ m$^{-4}$ s when $T_m$ is 300 K.

When the magnet is discharged through a dump resistor, the current decay is exponential with a decay time constant $\tau_1$ ($\tau_1 = L_1/R_{ex}$, where $R_{ex}$ is the resistance of the external dump resistor). The value of $F^*(T_m)$ at the magnet coil hot spot is given as follows:

$$F^*(T_m) = j_0^2 \frac{(r+1)}{\mathrm{r}} \left(\frac{\tau_1}{2} + t_{s0}\right) \qquad (11)$$

where $t_{s0}$ is the time needed to detect the quench and switch the resistor across the magnet coil (in most cases $t_{s0}$ is less than one second) and $j_0$ is the starting current density in the coil superconductor plus matrix material ($I_0$ divided by the conductor cross-sectional area). If a constant resistance dump resistor is used, the value of the resistance $R_e$ that results in a hot spot temperature less than or equal to $T_m$ can be expressed as follows:

$$R_e \geq \frac{j_0^2}{2F^*(T_m)} \frac{(r+1)}{r} L_1 \qquad (12)$$

The design value of $R_e$ should be larger than the value calculated by Eq. (12). For a constant resistance dump resistor, the maximum discharge voltage across the leads $V = R_e I_0$ will occur when the dump resistor is just put across the magnet.

Figure 3 shows a circuit diagram of the coil, its power supply, and the magnet dump circuit. A quench detection system is also shown. The values for inductances and $R$ given in Fig. 3 would apply to CASE 2 in Table 3. The quench detection system shown in Fig. 3 compares the voltage across the superconducting coil with the $dB/dt$ voltage due to changes in flux in the coil. If a voltage is measured across the coil and there is no corresponding $dB/dt$ voltage, there is a normal region in the coil. The normal region detected by the quench detector will open the switch, putting the dump resistor across the coil. Other methods can also be used to detect short normal sections within a magnet (65).

### The Role of Quench Back

It has been observed in most of the thin detector solenoid magnets that when the dump resistor is put across the electrical leads, the entire magnet becomes normal through the process of "quench back" (22). Quench back ensures that the coil current will decay faster than is predicted by the $L$ over $R_{ex}$ time constant. As a result, the magnet hot spot temperature is reduced.

There is a maximum time $t_Q$ before which quench back must occur in order to have quench back be a fail-safe method of quench protection (66,67). If the resistance of the external resistor induces quench back in a time less than the time $t_Q$, then the hot spot temperature is less than $T_m$, the maximum allowable hot spot temperature. The maximum allowable quench-back time $t_Q$ is the quench-back time required for fail safe quenching $t_F$ minus the time required for a heat pulse to cross the insulation between the quench back circuit (usually the coil support structure) and magnet coil $t_H$. (For a layer of ground plane insulation that is two millimeters thick, $t_H$ varies from 0.3 to 0.5 seconds depending on a number of factors.) For large detector solenoids, $t_H$ is usually small compared $\tau_1$. The value of $t_F$ can be determined using the following expression:

$$t_F = \frac{r}{r+1}\left[\frac{F^*(T_m) - F^*(T_s)}{j_0^2}\right] \tag{13}$$

where $r$ and $j_0$ are previously defined. $F^*(T_m)$ and $F^*(T_s)$ are defined by the right-hand term in Eq. (10) for the maximum hot spot temperature $T_m$ and the maximum temperature the coil would go to if the entire coil quenched instantaneously $T_s$. The value of $T_s$ depends on how the stored energy of the magnet is split between the hard aluminum support shell and the coil. For detector solenoids it is usually safe to split the magnet stored energy between the support shell and the coil according to their masses.

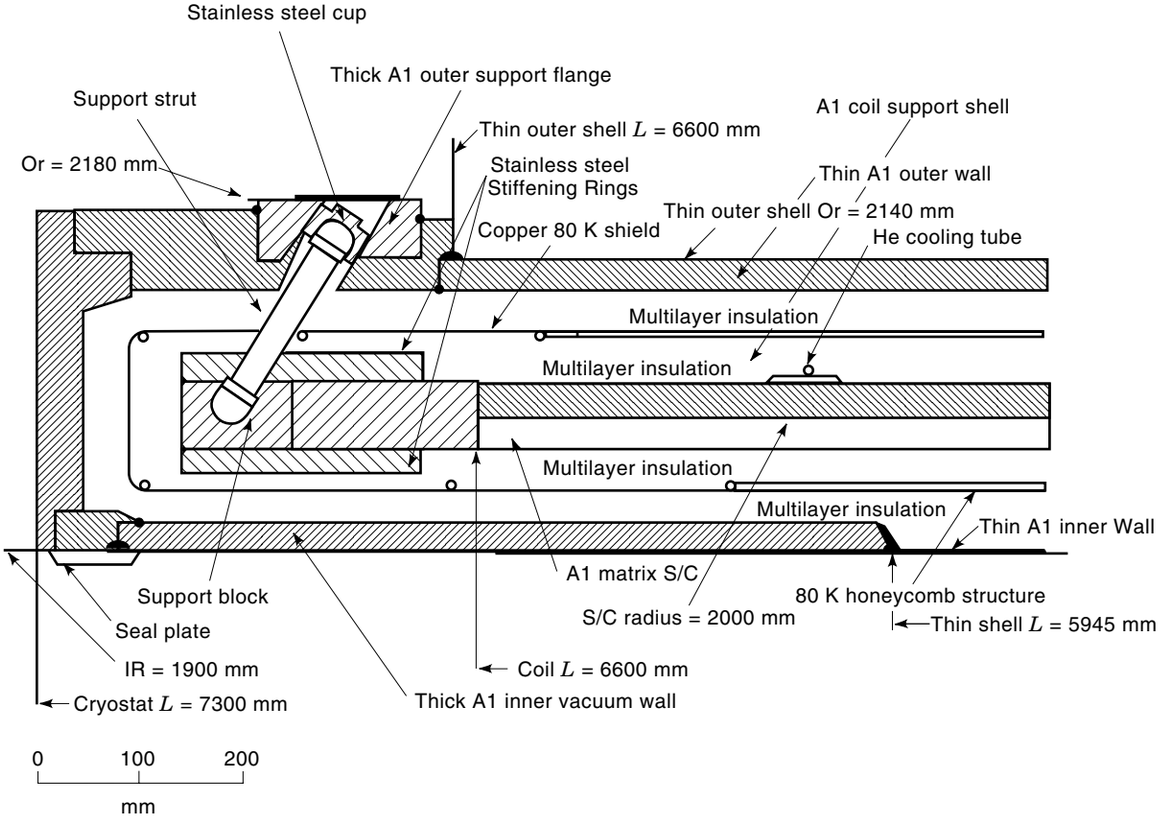


**Figure 2.** A cross section through the end of a 1.5 T thin solenoid with a 4.0 m coil diameter. A self-centering support strut is shown along with the stiff end ring for the superconducting coil package. (See Case 2 in Table 3.)

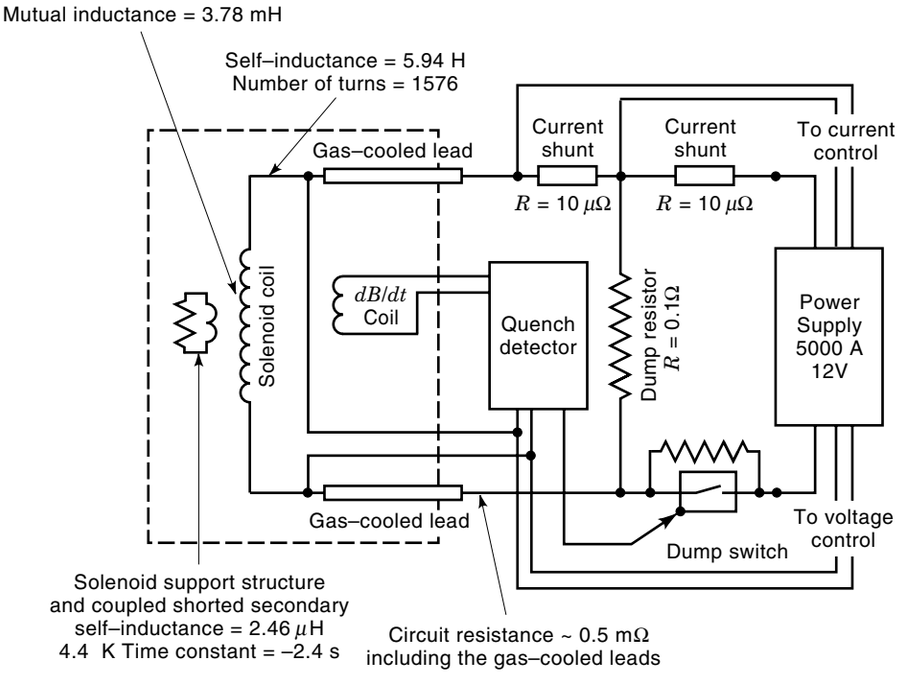


**Figure 3.** A schematic circuit diagram for the coil, power supply and quench protection circuit for a large detector solenoid with a support cylinder. (See Case 2 in Table 3.)

Once $t_Q$ has been determined, it is possible to calculate the resistance of an external resistor needed to cause the coil to quench back from the support tube in a time that is less than $t_Q$. The minimum resistance needed for quench back $R_m$ can be calculated using the following relationship for a solenoid coil that is well coupled inductively to its quench-back circuit (66):

$$R_m = \left(\frac{L_1}{\tau_2}\frac{N_2}{N_1}\frac{A_2}{I_0}\right)\left(\frac{\Delta H_2}{\rho_2 t_Q}\right)^{0.5} \tag{14}$$

where $L_1$ is the magnet coil self-inductance, $N_2$ is the number of turns in the quench-back circuit ($N_2 = 1$ when the support shell is the quench back circuit), $N_1$ is the number of turns in the magnet coil, $A_2$ is the cross-sectional area of the quench back circuit, $I_0$ is the coil current, $\Delta H_2$ is the enthalpy change per unit volume needed to raise the quench-back circuit temperature from 4 K to 10 K (for aluminum, $\Delta H_2 = 13{,}200$ J $m^{-3}$), $\rho_2$ is the resistivity of the quench-back circuit material, and $\tau_2$ is the $L$ over $R$ time constant for the quench-back circuit (the support tube).

If the minimum quench-back resistance $R_m$ is less than the resistance of the quench protection resistor $R_e$, quench back will always occur during a magnet dump. Therefore, the hot spot temperature of the coil is lower than $T_m$. When quench back is present, one can use a varistor (a resistor where the voltage across the resistor is nearly independent of current) as a dump resistor to speed up the quench process without increasing the coil voltages during the quench (68).

## DESIGN CRITERIA FOR THE ENDS OF A DETECTOR SOLENOID

The previous sections have dealt primarily with the center section of a detector solenoid. Much of the engineering for a detector solenoid is in the ends of the magnet, where thinness is not an issue. For example: (1) The support system for the solenoid cold mass is attached to the ends of the magnet. (2) The outside ends of the cryostat vessel are often where physical connections are made between the magnet and the rest of the detector. (3) The current leads and voltage taps into the coil will come out of the coil package at its ends. Gas-cooled electrical leads that connect the coil to the room-temperature outside world may also be located inside the magnet insulating vacuum vessel in the end region. (4) Cryogenic cooling is usually fed into the solenoid coil from the ends. Cooling should also include the intermediate temperature fluid (either liquid nitrogen at 80 K or helium gas at 50 to 80 K) used to cool the shields. (5) cryostat vacuum pumping ports will be located at the ends of the solenoid. (6) Room-temperature feed throughs for voltage taps, quench detection coils, temperature sensors, and pressure transducers will enter the magnet at the ends.

### Cold Mass Support System

The cold mass supports to room temperature must carry gravity forces, seismic forces, magnetic forces, and shipping forces. Most detector solenoids are designed to be at a neutral magnetic force point when the coil is at its operating temperature, so the cold mass support system must have a spring constant that is higher than the magnetic force constant.

Solenoids that are surrounded by iron are usually, but not always, in stable equilibrium in the radial direction and in unstable equilibrium in the axial direction. In the tortional direction (about the solenoid axis), there are almost no magnetic forces in a well-built solenoid, although asymmetric holes in the iron can introduce some of these forces. Stable equilibrium indicates that the magnetic forces will act in a direction that reduces a placement error; unstable equilibrium indicates that the magnetic forces will act in a direction

that increases the placement error. In the direction of stable equilibrium, the spring constant of the support system is not a critical issue except when determining how the magnet responds to vibration. In the direction of unstable equilibrium (usually the axial direction) the spring constant of the support system must be larger than the force constant for the magnet at its maximum design field. In general, the magnet force constant is linear with the location error and it increases with the magnet current squared. The magnetic force constant is a function of the design of the coil, the iron return yoke, and the pole pieces. Magnetic force constants will change as the iron in the magnetic circuit saturates.

Two types of cold mass support systems are commonly used in detector solenoids. The first is the self-centering support system where the position of the center of the solenoid coil does not change during the magnet cooldown or as the magnet is powered. The second support system carries axial forces with push–pull rods at one end of the magnet while the radial forces are carried by gravity support rods at both ends of the magnet. Both types of support systems must be designed to handle magnet shrinkage during the cooldown. A coil that is 6.6 m long and 4 m in diameter will shrink almost 28 mm in the axial direction and the radius will decrease about 8.4 mm. The external cryostat support system should be in line with the cold mass support system in order to avoid bending within the cryostat. The spring constant for the combined internal and external support systems must be greater than the magnetic force constant.

The self-centering support system has several advantages: (1) the position of the magnet center is the same both warm and cold. The PEP-4 solenoid magnetic center changed less than 0.3 mm during the magnet cooldown. (2) The radial and axial supports can be combined using either tension or compression rods. Two of the rods can also carry the tortional forces about the solenoid axis (tortional forces). The angle of the support rods can be set so that rod stress is not changed during the coil cooldown. (3) Since the axial spring constants must be high, the spring constant will be high in all directions. The self-centering support system will have a relatively high first mode vibration frequency. (4) The self-centering support system is robust in all directions, so earthquake and transportation forces should not be a problem.

The two disadvantages of the self-centering support system are as follows: (1) As the magnet coil cools down, it will move with respect to the ends of the cryostat vacuum vessel at both ends of the magnet. This movement must be considered when designing electrical leads, cryogen feed-throughs, and other attachments to the coil. (2) Flexure of the coil package (at the ends of the support cylinder) will affect the spring constant of the support system. The stiffness of the ends of the coil package and the number of radial–axial supports are the determining factors for the spring constant of this type of support system. Finite element stress and strain calculations can be used to determine the spring constant of the cold mass support system. A description of the design of a self centering support system can be found in Ref. 69. A location of a typical self-centering support compression strut for a detector solenoid is shown in Fig. 2. The strut rotates in its sockets as the solenoid cold mass contracts. The distance between the ball sockets does not change as the solenoid cools down from room temperature to 4 K. The angle of the strut with respect to the solenoid axis changes as the coil end of the strut moves toward the center of the solenoid.

### The Solenoid Support Structure, the Cryogenic Heat Sink

The support cylinder outside the superconducting winding serves the following functions: (1) The outer cylinder carries the magnetic pressure forces that are generated by the coil. (2) The outer cylinder transfers magnetic, gravitational, and seismic forces from the coil structure to the cold mass support system. (3) The outer cylinder carries the helium cooling tubes and acts as the heat sink for the coil and all attachments to it. This means that the outer support cylinder must be made from material that conducts heat well in both the radial and axial directions.

The end ring of the support cylinder should be as stiff as possible in bending. End-ring stiffness can be increased by making the ring thicker, thus increasing its moment of inertia, or one can fabricate a laminated end ring with a high elastic modulus material such as 304 stainless steel (elastic modulus of 200 GPa as compared to 69 GPa for aluminum) on the outside and the inside of the ring with aluminum in the center. The need for stiff end rings on the support cylinder is reduced as the number of cold mass supports per end is increased for a given coil diameter (69).

### Coil Electrical Connections and Leads to the Outside World

Connections to the superconducting coil that come through the end ring should be mounted on copper bus bars that are electrically insulated from the end rings. These bus bars should be cooled in liquid helium in order to avoid heat from outside the coil being deposited directly into the superconducting windings. Heat leaks down pulsed current leads, which are usually not gas cooled, can be particularly troublesome. The cooling circuit used to cool bus bars at the ends of the coil should be part of the magnet helium cooling system. Since much of the cooling circuit is electrically grounded, in-line electrical insulators will be required in the cooling lines that cool the electrical bus bars connected to the superconducting coil.

Most detector solenoids have gas-cooled electrical leads that are fed from a liquid helium pot located somewhere near the solenoid. The current buses between the lead pot and the coil are often cooled by conduction, a practice that has led to a number of failures. All current buses should be helium-cooled. The lead pot commonly used in detector magnets can be eliminated by using gas-cooled electrical leads that are attached to the ends of the coil structure. The helium used to cool these leads comes directly from the liquid helium cooling circuit. Gas-cooled leads attached to the end of the magnet are located within the cryostat vacuum, so these leads must be completely vacuum tight and they must withstand any increase in pressure that might occur in the cooling circuit during a quench (70). The bundled nested tube leads that were used on the PEP-4 experiment (71) and the g-2 solenoids (72) can be operated at any orientation within the cryostat vacuum vessel. Properly designed gas-cooled leads are stable and they are capable of operating for more than 30 min without gas flow.

## CRYOGENIC COOLING OF A THIN DETECTOR SOLENOID

Most of the detector solenoids shown in Table 1 are cooled by helium in tubes attached to the superconducting coil or the

support cylinder outside the coil. This technique has the following advantages over the bath cooling used for early cryostable detector magnets (73): (1) Tubular cooling eliminates the cryostat helium vessels. As a result, the solenoids are thinner and less massive. (2) The volume of helium in a tubular cooling system is small. Once this helium is evaporated during a quench, it is expelled from the tube. Large quantities of helium gas are not produced during a magnet quench. The helium expelled during a magnet quench can be returned to the refrigerator where it is recovered. (3) Tubes can withstand high pressures during a quench. Relief valves for the system can be moved from the magnet cryostat to the helium supply system, which can be outside the detector. (4) Magnet cooldown can be done directly using the helium refrigerator. (5) Recovery from a quench can be simplified using a well-designed tubular cooling system.

Detector magnets are cooled with two-phase helium rather than supercritical helium for the following reasons: (1) The operating temperature for the superconducting solenoid is lower (18). As two-phase helium flows down the cooling circuit, it gets colder as its pressure goes down. The temperature of a single-phase cooling circuit increases as one goes along the cooling circuit. (2) The mass flow through the cooling circuit is minimized. As a result, the pressure drop along the flow circuit is lower. (3) There is no need for auxiliary helium pumping in a two-phase flow circuit. Helium flow can be provided directly by the J-T circuit of the refrigerator. (4) A properly designed two-phase helium flow system can be operated at heat loads greater than the capacity of the refrigerator for a period of time. Thus fluctuations in the heat load can be tolerated by two-phase flow circuits that are designed for the average heat load. The most often stated disadvantage of two-phase cooling is the potential existence of flow and pressure fluctuations in the cooling tube. This has not been a problem in detector magnets when the two-phase helium cooling circuit is properly designed. Experiments with extensively looped cooling tubes that are hundreds of meters long have shown that proper design of the flow circuit can nearly eliminate the flow oscillation problem (73,74).

The types of two-phase helium flow circuits are commonly used in detector solenoids are the forced two-phase flow system and the natural convection two-phase flow system. Forced two-phase flow is appropriate when the flow circuits are long and when the control dewar is below the top of the magnet. Natural convection two-phase flow is appropriate when there is a large vertical head between the helium dewar and the load and when there are many parallel flow circuits so that the mass flow in any one circuit can be kept low. Either type of two-phase helium flow circuit can be made to work in most detector solenoids.

The key to stable operation of forced two-phase helium cooling circuits is the control dewar and heat exchanger (25,73). Flow for the magnet cooling circuit comes from the J-T circuit of the helium refrigerator. Cooling flow can also come from a positive displacement helium pump (75), but allowances must be made for the pump work heating generated by such a pump. Two-phase flow from the refrigerator J-T circuit flows through a heat exchanger that is cooled in a bath of liquid helium at the suction pressure of the cold end of the refrigerator. The temperature of the helium bath is the lowest

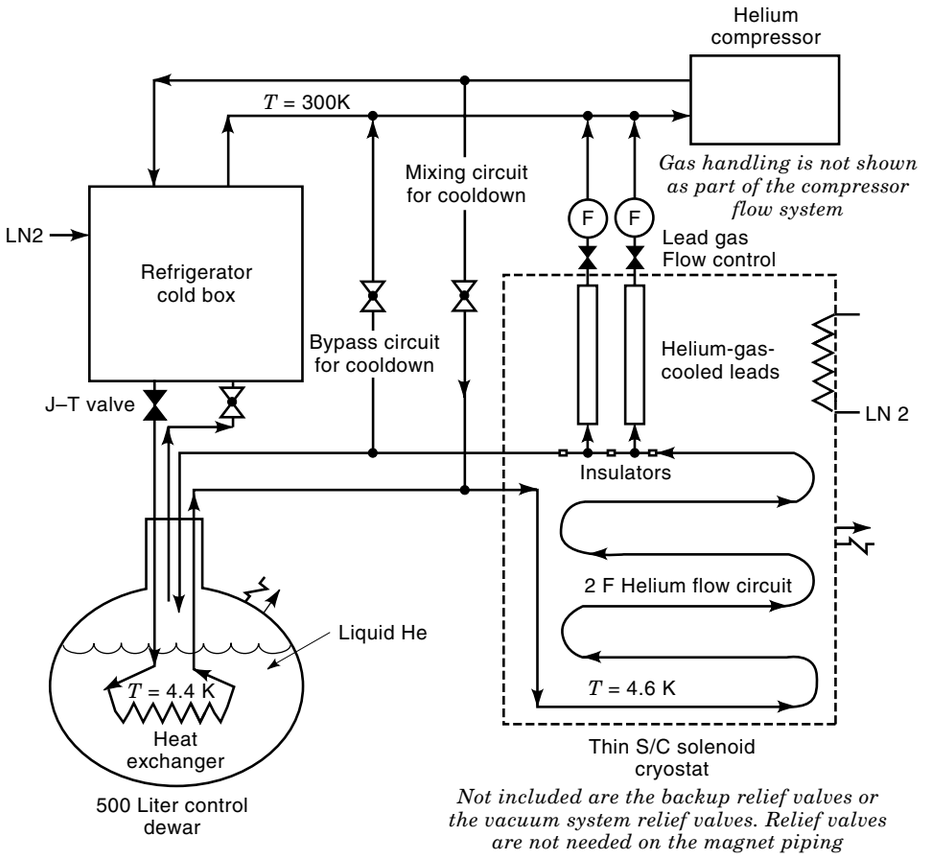


**Figure 4.** A schematic representation of a forced two-phase helium cooling system for a large detector solenoid while the solenoid is cold. (*Note:* Open valves are unshaded; closed valves are shaded. Dark lines carry flow; shaded lines carry no flow.)

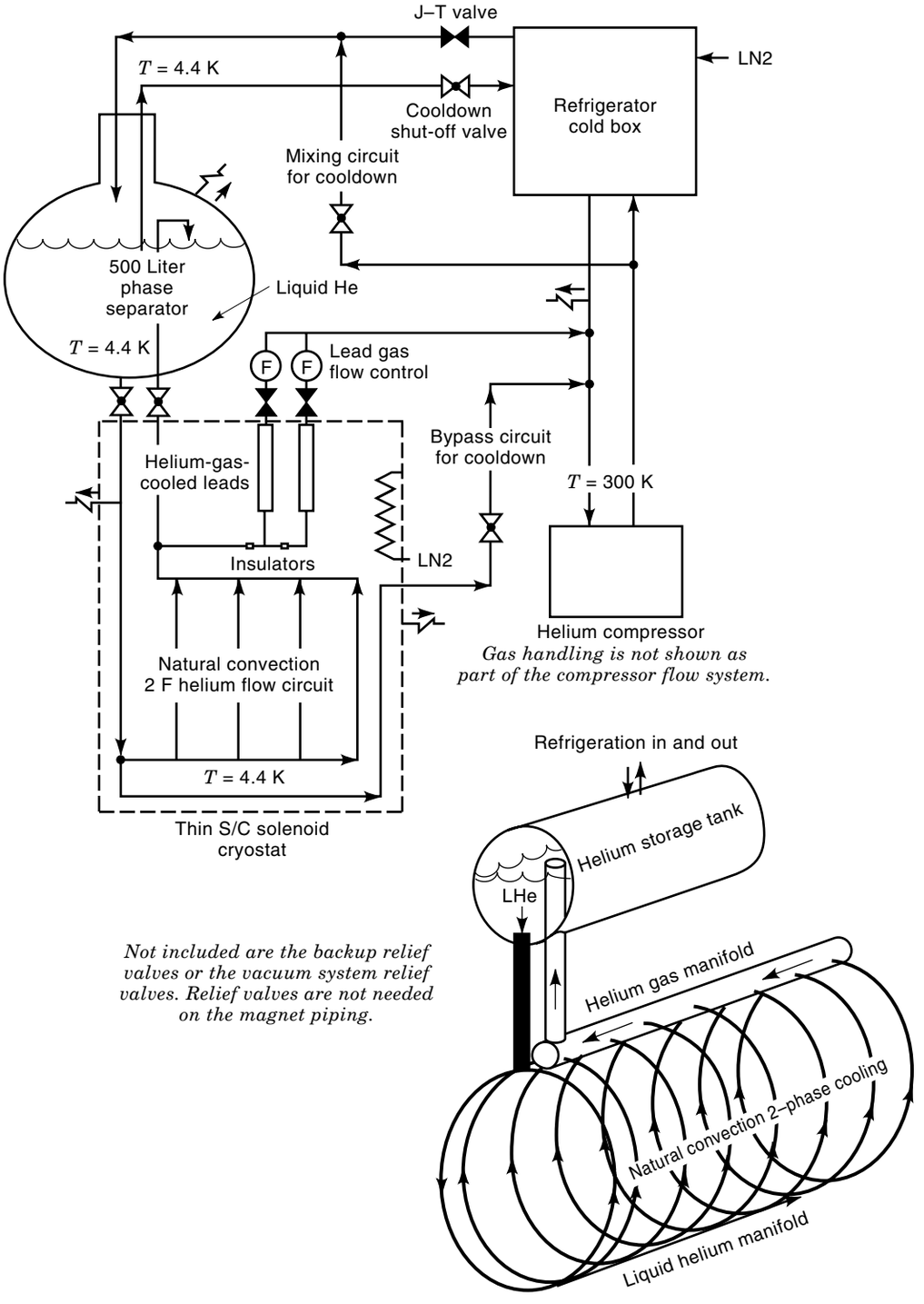


**Figure 5.** A schematic representation of a natural convection two-phase helium cooling system for a large detector solenoid while the solenoid is cold. (The insert at the lower right shows the physical arrangement of the natural convection cooling system.)

temperature in the two-phase flow circuit. Within the heat exchanger, helium in the gas phase is condensed to liquid so that the helium leaving the heat exchanger either is on the saturated liquid line or is slightly subcooled. As a result, the average density of the helium in the flow circuit is maximized, which will cause the flow pressure drop through the flow circuit to be reduced a factor of two or three as compared to the same flow circuit without a heat exchanger in the helium bath. The use of the heat exchanger in the control dewar allows the operation of the cooling circuit with a heat flow into the magnet that exceeds the capacity of the refrigerator by as much as 50%. Under this condition, the magnet can be

kept cold as long as the heat exchanger in the control dewar is kept covered with liquid helium. The control dewar enhances flow circuit stability. Figure 4 shows a schematic representation of a forced two-phase helium cooling circuit in its simplest form. The valves in Fig. 4 are shown as they would be when the magnet is operating at 4 K.

The advantages of forced two-phase cooling are as follows: (1) The entire detector solenoid can be cooled using a single helium flow circuit. As a result, the cooldown of the magnet is straight forward because all of the sensible heat of the helium can be employed during the cooldown process. (2) The operating temperature for a two-phase cooled magnet is lower than it would be for any supercritical helium-cooled magnet. (3) The control dewar with its heat exchange can be located flexibly with respect to the magnet coil. Transfer lines to and from the coil can be long, if desired. (4) Gas-cooled electrical leads and shields can be cooled directly from the two-phase cooling circuit. The connections for leads and shields can be made inside the magnet cryostat vacuum vessel. (5) Since the liquid helium inventory in contact with the magnet is limited to the helium in the cooling tube, the amount of helium gas produced during a quench is small. (6) The liquid helium in the control dewar can be used to speed up the recovery of the superconducting magnet after a quench. The primary disadvantage of forced two-phase cooling is that when the refrigerator stops, the magnet cooling stops. The magnet will quench within minutes after the refrigerator stops running. For some users this is a serious consideration.

The natural convection two-phase cooling system overcomes the primary disadvantage of a forced two-phase cooling system in that the magnet will remain cold and operating even when the refrigerator is not in operation. The cooling for a natural convection cooling system comes from the helium that is stored in a tank that is above the top of the coil. The greater the head between the storage tank and the top of the magnet, the better the natural convection two-phase flow system operates. In order for the natural convention flow system to operate effectively, the following conditions must be present: (1) The pipe from the bottom of the helium storage dewar to the manifold at the bottom of the magnet should be short and well-insulated. There should be no boiling in helium transferred to the lower manifold on the coil package. (2) In order to reduce the flow circuit pressure drop, there should be many short up-flow circuits in parallel going up and around the coil to the manifold at the top of the magnet. Boiling should occur in these tubes. This increases the helium flow through the cooling system. (3) The pipe from the manifold at the top of the coil package should dump two-phase helium into the top of the storage tank, where phase separation occurs. This pipe should be insulated from the helium that is in the storage tank. The difference in helium density in the pipe connecting the tank and the lower manifold and the two-phase helium in the cooling tubes circling the magnet provides the driving force for the flow circuit. Figure 5 shows a schematic representation of a natural convection two-phase helium cooling circuit in its simplest form. The upper part of Fig. 5 shows a schematic of how the refrigerator, its compressors, and the magnet would be hooked up. The lower part of Fig. 5 shows the physical arrangement of the helium storage tank (phase separator) and the detector solenoid. The storage tank shown in Fig. 5 is 500 liters, but that tank could be much larger if needed. The valves in Fig. 5 are shown as they would be when the magnet is operating at 4 K.

Natural convection flow has some disadvantages, which are as follows: (1) Cooldown of the magnet is not as straightforward as with the forced two-phase cooling system. This difficulty can be overcome by having a separate forced flow circuit for the magnet cooldown. (2) In a natural convection cooled magnet system, all of the helium that is in the storage tank may be boiled during a magnet quench. This can be overcome by installing an automatic shut-off valve, which is triggered by the quench detector, in the pipe between the storage tank and the liquid helium manifold on the bottom of the magnet. (3) The thin section of the solenoid has a larger radiation thickness top and bottom in the regions where the liquid helium and two-phase helium manifolds are located. (4) The helium storage tank for natural convection cooling must be located directly above the magnet coil, and the transfer lines between the storage tank and the coil should be as short as possible. The physics experiment must accommodate these transfer lines.

## BIBLIOGRAPHY


1. J. E. Kunzler et al., *Phys. Rev. Lett.,* **6**: 89, 1961.
2. R. C. Wolgast et al., Superconducting critical currents in wire samples and some experimental coils, in *Advances in Cryogenic Engineering,* Vol. 8, New York: Plenum Press, 1962, p. 38.
3. C. Laverick, The performance characteristics of small superconducting coils, in *Advances in Cryogenic Engineering,* Vol. 10, New York: Plenum Press, 1964, p. 105.
4. Z. J. J. Stekly and Z. L. Zar, Stable superconducting coils, *IEEE Trans. Nucl. Sci.,* **NS-12**: 367, 1965.
5. J. R. Purcell, The 1.8 tesla, 4.8 m bubble chamber magnet, *Proc. 1968 Summer Study Superconducting Devices Accelerators,* BNL 50155 (C-55), p. 765, 1968.
6. R. E. Jones et al., Construction of the 12 foot bubble chamber superconducting magnet cryostat, in *Advances in Cryogenic Engineering,* Vol. 15, New York: Plenum Press, 1969, p. 141.
7. D. P. Brown, R. W. Burgess, and G. T. Mulholland, The superconducting magnet for the Brookhaven National Laboratory 7 foot bubble chamber, in *Proc. 1968 Summer Study Superconducting Devices Accelerators,* BNL 50155 (C-55), p. 794, 1968.
8. E. G. Pewitt, Superconductivity in high energy physics, in *Advances in Cryogenic Engineering,* Vol. 16, New York: Plenum Press, 1970, p. 19 (a review of large magnets).
9. E. V. Haebel and F. Wittgenstein, *Proc. Int. Conf. Magnet Technol.,* Hamburg, Germany, 1970.
10. T. H. Fields, Superconductivity applications in high energy physics, *IEEE Trans. Magn.,* **MAG-11**: 113, 1975.
11. M. Morpurgo, Construction of a superconducting test coil cooled by helium forced circulation, *Proc. 1968 Summer Study Superconducting Devices Accelerators,* BNL 50155 (C-55), 953, 1968.
12. M. Morpurgo, *Proc. Int. Conf. Magnet Technol.,* Hamburg, Germany, 1970.
13. C. P. Bean et al., Research Investigation of the Factors that Affect the Superconducting Properties of Material, AFML-TR-65-431, Air Force Materials Laboratory, Wright Patterson Air Force Base, Ohio, 1965.
14. R. Hancox, *Phys. Lett.,* **16**: 208, 1965.
15. P. F. Chester, *Rep. Prof. Phys.,* **30** (2): 361, 1967.
16. P. F. Smith and J. D. Lewin, Pulsed superconducting synchrotrons, *Nucl. Instr. Methods,* **52**: 248, 1967.

17. M. N. Wilson et al., Experimental and theoretical studies of filamentary superconducting composites, Part 1: Basic ideas and theory, *J. Phys. Appl. Phys.,* **3**: 1517, 1970.
18. M. A. Green, Cooling intrinsically stable superconducting magnets with super-critical helium, *IEEE Trans. Nucl. Sci.,* **NS-18**: 664, 1971.
19. H. Desportes, Superconducting magnets for accelerators, beam lines and detectors, *IEEE Trans. Magn.,* **MAG-17**: 1560, 1981.
20. M. A. Green, Large superconducting solenoid for the MINIMAG experiment, in *Advances in Cryogenic Engineering,* Vol. 21, New York: Plenum Press, 1975, p. 24.
21. P. H. Eberhard et al., Tests on large diameter superconducting solenoids designed for colliding beam accelerators, *IEEE Trans. Magn.,* **MAG-13**: 78, 1977.
22. M. A. Green, The Development of Large High Current Density Superconducting Solenoid Magnets for Use in High Energy Physics Experiments, LBL-5350, doctoral dissertation, UC Berkeley, May 1977.
23. M. A. Green, Large superconducting detector magnets with ultra thin coils for use in high energy accelerators and storage rings, *Proc. 6th Int. Conf. Magnet Technol.,* Bratislava, Czechoslovakia, p. 429, 1977.
24. P. H. Eberhard et al., A magnet system for the time projection chamber at PEP, *IEEE Trans. Magn.,* **MAG-15**: 128, 1979.
25. M. A. Green, W. A. Burns, and J. D. Taylor, Forced two-phase helium cooling of large superconducting magnets, in *Advances in Cryogenic Engineering,* Vol. 25, New York: Plenum Press, 1979, p. 420.
26. J. Benichou et al., Long term experience on the superconducting magnet system for the CELLO detector, *IEEE Trans. Magn.,* **MAG-17**: 1567, 1981.
27. J. M. Royet, J. D. Scudiere, and R. E. Schwall, Aluminum stabilized multifilamentary Nb-Ti conductor, *IEEE Trans. Magn.,* **MAG-19**: 761, 1983.
28. E. Leung et al., Design of an indirectly cooled 3-m diameter superconducting solenoid with external support cylinder for the Fermilab collider detector facility, *IEEE Trans. Magn.,* **MAG-19**: 1368, 1983.
29. A. Wake et al., A large superconducting thin solenoid magnet TRISTAN experiment (VENUS) at KEK, *IEEE Trans. Magn.,* **MAG-21**: 494, 1985.
30. H. Hirabayashi, Detector magnets in high energy physics, *IEEE Trans. Magn.,* **MAG-24**: 1256, 1988.
31. K. Tsuchiya et al., Testing of a 3 tesla superconducting magnet for the AMY detector at Tristan, in *Advances in Cryogenic Engineering,* Vol. 33, New York: Plenum Press, 1987, p. 33.
32. J. M. Baze et al., Design, construction and test of the large superconducting solenoid ALEPH, *IEEE Trans. Magn.,* **MAG-24**: 1260, 1988.
33. R. Q. Apsey et al., Design of a 5.5 meter diameter superconducting solenoid for the DELPHI particle physics experiment at LEP, *IEEE Trans. Magn.,* **MAG-21**: 490, 1985.
34. P. T. M. Clee, Rutherford Appleton Laboratory, Didcot, United Kingdom, private communication.
35. A. Bonito Oliva et al., Zeus thin solenoid: Test results analysis, *IEEE Trans. Magn.,* **MAG-27**: 1954, 1991.
36. D. Andrews, Oxford Technology Ltd., Oxford, United Kingdom, private communication.
37. C. M. Monroe et al., The CLEO II Magnet—design, manufacture and tests, *Proc. Twelfth Int. Cryogenic Eng. Conf.,* Southampton, United Kingdom, Guildford, United Kingdom: Butterworth, 773, 1988.
38. A. Yamamoto et al., Development of a prototype thin superconducting solenoid magnet for the SDC detector, *IEEE Trans. Appl. Supercond.,* **5**: 849, 1995.
39. T. Mito et al., Prototype thin superconducting solenoid for particle astrophysics in space, *IEEE Trans. Magn.,* **MAG-25**: 1663, 1989.
40. Y. Makida et al., Ballooning of a thin superconducting solenoid for particle astrophysics, *IEEE Trans. Appl. Supercond.,* **5**: 658, 1995.
41. P. Fabbricatore et al., The superconducting magnet for the BaBar detector of the PEP-II B factory at SLAC, *IEEE Trans. Magn.,* **MAG-32**: 2210, 1996.
42. J. M. Baze, Progress in the design of a superconducting toroidal magnet for the ATLAS detector on LHC, *IEEE Trans. Magn.,* **MAG-32**: 2047, 1996.
43. D. E. Baynham et al., Design of the superconducting end cap toroids for the ATLAS experiment at LHC, *IEEE Trans. Magn.,* **MAG-32**: 2055, 1996.
44. F. Kircher, H. Deportes, and B. Gallet et al., Conductor developments for the ATLAS and CMS magnets, *IEEE Trans. Magn.,* **MAG-32**: 2870, 1996.
45. G. Bunce et al., The large superconducting solenoids for the g-2 muon storage ring, *IEEE Trans. Appl. Supercond.,* **5**: 853, 1995.
46. G. Bunce et al., Test results of the g-2 superconducting solenoid magnet system, *IEEE Trans. Appl. Supercond.,* **7**: 626, 1997.
47. *Review of Particle Properties,* compiled by the Particle Data Group, *Rev. Mod. Phys.,* **48** (2): Part II, 50, 1978.
48. Y. S. Tsai, Pair Production and Bremsstrahlung of Charged Leptons, SLAC-PUB-1365, Table III.6, 1974.
49. W. R. Smythe, *Static and Dynamic Electricity,* 2nd ed., New York: McGraw-Hill, 1950.
50. POISSON/SUPERFISH Reference Manual, LANL Publication LA-UR-87-126, 1987.
51. Part of the TOSCA series of programs produced by Vector Fields Ltd., Oxford, United Kingdom.
52. M. A. Green, Calculating the $J_c$, $B$, $T$ surface for niobium titanium using the reduced state model, *IEEE Trans. Magn.,* **MAG-25**: 2119, 1989.
53. B. J. Maddock and G. B. James, Protection and stabilization of large superconducting coils, *Proc. IEE,* **115** (4): 543, 1968.
54. P. H. Eberhard et al., Quenches in large superconducting magnets, In *Proc. 6th Int. Conf. Magnet Technol.,* Bratislava, Czechoslovakia, 654, 1977.
55. M. A. Green, Quench back in thin superconducting solenoid magnets, *Cryogenics,* **24**: 3, 1984.
56. A. Yamamoto et al., A thin superconducting solenoid with the internal winding method for collider beam experiments, in *Proc. 8th Int. Conf. Magnet Technol.,* September 1983.
57. A. Yamamoto et al., Design study of a thin superconducting solenoid for the SDC detector, *IEEE Trans. Appl. Supercond.,* **3**: 95, 1993.
58. R. J. Roark and W. C. Young, *Formulas for Stress and Strain,* 5th ed., New York: McGraw-Hill, 1975.
59. S. Timoshenko, *Theory of Plates and Shells,* New York: McGraw-Hill, 1940.
60. H. E. Sauders and D. F. Wittenberg, Strength of thin cylindrical shells under external pressure, *ASME Trans.,* **53**: 207, 1931.
61. E. P. Popov, *Mechanics of Materials,* Englewood Cliffs, NJ: Prentice-Hall, 1959.
62. ASME Boiler and Pressure Vessel Code, Section 8, Division 1, ANSI/ASME BPV-VIII-1.

63. R. Fast et al., Isogrid vacuum shell for large superconducting solenoids, in *Advances in Cryogenic Engineering,* Vol. 39, New York: Plenum Press, 1993, p. 1991.

64. H. Yamaoka et al., Development of a brazed-aluminum-honeycomb vacuum vessel for a thin superconducting solenoid magnet, in *Advances in Cryogenic Engineering,* Vol. 39, New York: Plenum Press, 1993, p. 1983.

65. M. N. Wilson, *Superconducting Magnets,* Oxford, United Kingdom: Oxford Clarendon Press, 1983, p. 219.

66. M. A. Green, The role of quench back in the quench protection of a superconducting solenoid, *Cryogenics,* **24**: 659, 1984.

67. M. A. Green, PEP-4, TPC Superconducting Magnet, A Comparison of Measured Quench Back Time with Theoretical Calculations of Quench Back Time for Four Thin Superconducting Magnets, Lawrence Berkeley Laboratory Report LBID-771, August 1983, unpublished.

68. J. D. Taylor et al., Quench protection for a 2 MJ magnet, *IEEE Trans. Magn.,* **MAG-15**: 855, 1979.

69. M. A. Green, PEP-4, Large Thin Superconducting Solenoid Magnet, Cryogenic Support System Revisited, Lawrence Berkeley Laboratory Engineering Note M5855, March 1982, unpublished.

70. M. A. Green, Calculation of the pressure rise in the cooling tube of a two phase cooling system during a quench of an indirectly cooled superconducting magnet, *IEEE Trans. Magn.,* **MAG-30**: 2427, 1994.

71. R. G. Smits et al., Gas-cooled electrical leads for use on forced cooled superconducting magnets, *Advances Cryogenic Eng.,* Vol. 27, New York: Plenum Press, 1981, p. 169.

72. M. A. Green et al., A design method for multi-tube gas cooled electrical leads for the g-2 superconducting magnets, in *Advances in Cryogenic Engineering,* Vol. 41, New York: Plenum Press, 1996, p. 573.

73. M. A. Green et al., The TPC Magnet Cryogenic System, Lawrence Berkeley Laboratory Report LBL-10552, May 1980, unpublished.

74. J. D. Taylor and M. A. Green, Garden Hose Test, Lawrence Berkeley Laboratory, Group A Physics Note 857, November 1978, unpublished.

75. W. A. Burns et al., The construction and testing of a double-acting bellows liquid helium pump, *Proc. 8th Int. Cryogenics Eng. Conf.,* Genova, Italy, Guildford, United Kingdom, IPC Science and Technology Press, 383, 1980.

MICHAEL A. GREEN
Lawrence Berkeley National
Laboratory